

GPPS-TC-2022-0067

Economically and Aerodynamically Optimized Closure of Wind Tunnel Test Sections

Konrad M. Hartung

Jade University of Applied Sciences

konrad.hartung@jade-hs.de

Wilhelmshaven, Lower Saxony, Germany

Dennis M. Sanders

Jade University of Applied Sciences

dennis.sanders@jade-hs.de

Wilhelmshaven, Lower Saxony, Germany

Karsten Oehlert

Jade University of Applied Sciences

karsten.oehlert@jade-hs.de

Wilhelmshaven, Lower Saxony, Germany

ABSTRACT

For high-lift models like airfoils for wind turbines, aircraft or turbomachinery applications wind tunnel measurements in open test sections are often unsuitable for determining precise lift and drag coefficients as streamwise gradients and the imposed ambient pressure boundary condition at the shear layer of the free jet can lead to a deviation of the local base pressure. Therefore, based on the existing closed circuit wind tunnel Göttingen-Type with circular cross-section at the Jade University of Applied Sciences, the authors present an approach for an economically and aerodynamically optimized closure of the wind tunnel test section. For ease of installing models and measurement instrumentation as well as optical accessibility the cross-section of the test section was chosen to be square shaped. With the objective to keep the numbers of new components to be manufactured manageable the transition of the cross-sectional shape from round to square has been embedded into the designed nozzle geometry. For the investigation on its effect on the homogeneity of the flow quantities, numerical simulations of a simplified wind tunnel model were conducted. In total, three different setups have been considered, including a setup with fully circular and mostly square shaped cross-sections for comparison. The evaluation was carried out based on the percentage velocity variation on a fixed number of evaluation planes within the test section. The results show that the financially most reasonable setup also positively affects the flow homogeneity in the closed test section. With the outlined design approach an overall higher flow homogeneity can be achieved compared to a setup with a fully square cross-section. Further as a lower energy demand for operation can be expected due to lower pressure losses of circular shaped flow guiding components a corresponding setup is economical beneficial .

INTRODUCTION

Despite the continuous improvement of computational capability numerical methods have still not reached a sufficient level to entirely replace the need for experimental data. Therefore wind tunnel test facilities are still a necessary and powerful tool for flow investigations on a variety of applications in laboratory scales. Basically two types of wind tunnel designs exist, whereby additionally it is distinguished between configurations with open and closed test sections. Open circuit wind tunnels are characterized by an essentially straight flow path. The entering air flow passes through a contraction as well as an open (Eiffel-Type) or closed (NPL-Type) test section followed by a diffuser and a fan section before exiting again. In contrast the air flow in closed circuit wind tunnels (Prandtl-, Göttingen-Type) recirculates continuously through a series of ducts and turning vanes, whereby again the tunnel may exhibit either a closed or open test section (Barlow et al., 1999). As there are numerous advantages and disadvantages associated with open and closed circuit configurations the type chosen in general depends on the financial resources available and operational purpose. Nonetheless one can summarize that in case of open circuit wind tunnels the flow quality may be affected by in room activities or the weather when open to the atmosphere whereby closed circuit wind tunnels enable consistently well controlled flow quality. Further for a given

size and speed open circuit tunnels in general require a higher energy demand in comparison to closed circuits whereas the constructional cost usually turns out to be lower. In case of high utilization or long measuring times however closed circuit wind tunnels may require some sort of additional cooling system to counteract the temperature rise induced by energy dissipation (Barlow et al., 1999). No less influential is the choice of the test section configuration itself. While closed test sections enable consistently good flow quality they require a higher blockage correction with increasing model to cross-section area ratio (Barlow et al., 1999; Chen and Liou, 2011). Further the presence of walls hamper the access for traversing and probe devices and may evoke local leakages. Open test sections on the other hand are minor influenced by blockage effects and therefore allow the use of larger test models but may suffer from insufficient flow quality. Especially for high-lift models measurements in open test section configurations are often unsuitable for determining precise lift and drag coefficients. Their usage may lead to a drastic deviation of the local base pressure (Wetzel et al., 2013; Kramer et al., 1986) which contributes essentially to the aerodynamic drag. According to the expertise of the authors the deviations can be mainly attributed to three reasons. The blockage effect in closed test section configurations causes a slight increase of the velocity and therefore a slight decrease of the local base pressure in comparison to open test section configurations. Further divergent static pressure gradients in flow direction may cause deviating base pressures. However, the deviation is most strongly influenced by the different pressure boundary conditions imposed by the test section configuration. Closed test sections impose a zero pressure gradient at the walls while in case of open test section the atmosphere pressure of the ambient air is imposed at the shear layer of the free jet. The former clearly corresponds more to the case of undisturbed natural flow. Additionally the absence of walls can provide serious wake deflection problems especially for higher angles of attack and thus adversely affect the validity of wake measurements. To circumvent the undesired side-effects and the costly correction procedures associated with open test sections the authors present within this study an approach for an economically and aerodynamically optimized closure of wind tunnel test sections.

METHODOLOGY

Starting point for the investigations is the 7 m long and 3 m wide closed circuit wind tunnel Göttingen-Type with circular cross section at the Jade University of Applied Sciences. The open test section exhibits an cross sectional area of $\pi \cdot (0.25 \text{ m})^2$ and a variable length in the limits between $1.75 \cdot D$ and $2.00 \cdot D$ (Figure 1). For the upcoming investigations on drag affecting surface structures by wake measurements the test section shall be closed to enable precise measurements of aerodynamic drag coefficients. According to the requirements the following design criteria were defined:

- The length of the closed-circuit wind tunnel may not exceed 10 m.
- The maximum velocity of the open test section configuration must be achieved (44.5 m/s with a turbulence level of around 1% at the test section inlet), enabling measurements at a Reynolds number of approximately $5e5$ based on the airfoil chord length.
- The contraction ratio $C_R = A_1/A_2$ specified by the contraction inlet A_1 and outlet A_2 plane shall be at least maintained or increased in comparison to the open test section configuration ($C_R \approx 6.1$).
- High flow homogeneity in the test section is aspired.
- The number of new components to be manufactured should be minimized.
- The length of the test section must be at least $l_{test} = 2 \cdot d_h$.
- The cross-sectional area of the test section must be square shaped and optically accessible.

As for ease of installing models and measurement instrumentation as well as optical accessibility the cross-section of the closed test section was chosen to be square shaped a transition of the cross-sectional shape must be provided additionally. According to the state of the art, the transition of the cross-sectional shape usually takes place in the immediate vicinity of the drive system with the aid of shape adapters. However, following this approach the wind tunnel modification would have been equivalent to a new construction. Therefore a alternative location for a aerodynamically reasonable and financially affordable cross-sectional transition was indispensable. Financially optimal would be a cross-sectional transition within the nozzle geometry, as this reduces the number of new components to be manufactured to a minimum. Furthermore, as with this setup most components retain their circular cross-sectional shape, which causes less pressure losses, a notable decreased energy demand can be expected. Figure 2 shows the corresponding wind tunnel configuration where the parts 6.0 nozzle, 7.0 test section and 8.0 second diffuser were redesigned. The extension of the diffuser as well as the additional extensions, parts 1.1 and 1.2 were necessary in order to bridge the slightly different dimensions of the diffuser inflow and the nozzle outflow cross section, which is typically for open test section configurations. From the aerodynamic perspective a cross-sectional transition within the nozzle geometry also seems reasonable. On the one hand, a local widening and therefore additional separation regions in the corner areas of shape adapters can be avoided during transition. On the other hand, by embedding the cross-sectional change within the nozzle the undesired flow acceleration in the corner regions of the contraction section with rectangular cross section due to the intersecting circumferential edges can be minimized. As there are no literature data available for the impact of a comparable nozzle geometry on the flow homogeneity, the impact is investigated numerically within the scope of this study.

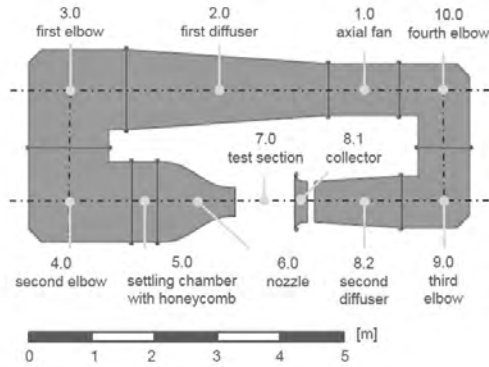


Figure 1 Wind tunnel Göttingen-Type open test section configuration

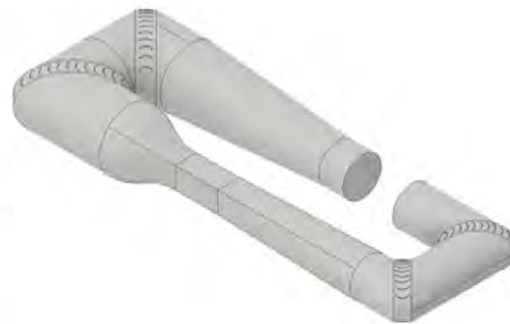
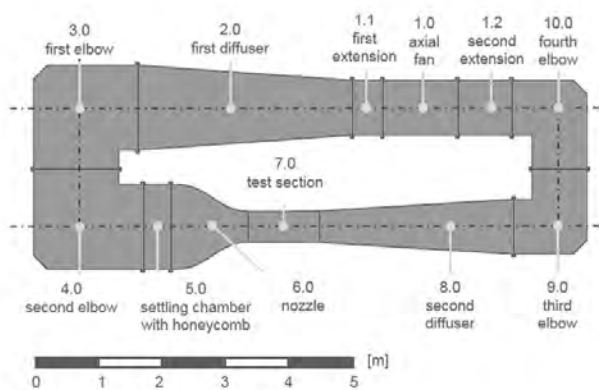


Figure 2 Wind tunnel Göttingen-Type closed test section configuration

Numerical Methods

In total, three different setups have been considered for the investigation including a setup with fully circular and mostly square shaped cross-section. The results are compared to a setup with a transitional cross-sectional shape from round to square which is embedded within the nozzle geometry. For the comparison of these three setups a simplified wind tunnel model is used. This model consists of an inflow tube, a nozzle, a test section, a diffuser and an outflow tube as shown in (Figure 3A). To ensure that the velocity and turbulence fields are fully developed before entering the contraction, the inflow tube length is set to $100 \cdot D$. Furthermore the length of the outflow tube is set to $12 \cdot D$ to prevent backflow influence in the test section. In addition for all simulations an uniform length for the test section and contraction was specified in the size of $0.9m$ and $1.2m$ respectively. Table 1 summarizes the cross-sectional shapes for all three setups at the in- and outflow of the individual components. For these positions the cross sectional areas have the same size independent of the considered setup. All three cases have a circular shaped cross-section at the diffuser outlet as this is required for the connection to

Table 1 Geometric specifications for the wind tunnel setups

| Component Nr. | Position | Circular Setup | Square Setup | Transitional Setup |
|---------------|-----------------|----------------|--------------|--------------------|
| - | inflow pipe | circular | square | circular |
| 6.0 | nozzle inlet | circular | square | circular |
| 6.0 | nozzle outlet | circular | square | square |
| 7.0 | test section | circular | square | square |
| 8.0 | diffuser inlet | circular | square | square |
| 8.0 | diffuser outlet | circular | circular | circular |
| - | outflow pipe | circular | circular | circular |

the drive system. Furthermore the test sections for all three setups contain a slight widening of the cross-sectional area to counteract the flow acceleration due to boundary layer thickening. To reduce the computational costs only a quarter of the geometry is used for the numerical simulations. The geometry is generally meshed with unstructured poly-hexcore cells.

At the wall prism layers are used to improve the boundary layer resolution. To ensure the independence of the solution from the mesh a grid independence study was carried out. Overall three meshes with a total number of 140k, 850k and 5.5 million cells were used. For the evaluation the percentage velocity variation outlined in the section flow homogeneity was applied. Accordingly the mesh with the medium resolution illustrated in (Figure 3B) was sufficient and hence is applied for further investigations. The simulations were performed using the realizable- $k-\epsilon$ RANS-model with near wall treatment in Ansys fluent. For the near wall regions the Menter-Lechner boundary layer function, which is insensitive towards varying y^+ values, was used. The y^+ values achieved for the full domain in the range of $30 < y^+ < 200$ were therefore acceptable. As boundary conditions a velocity inlet and a pressure outlet are specified. Furthermore the no slip condition is applied for all walls and symmetry boundaries are used for the quartered geometry. As fluid air under atmospheric conditions is specified, which is assumed to be incompressible due to low Mach numbers. The solution is calculated with a coupled solver and converged residuals below $1e-9$.

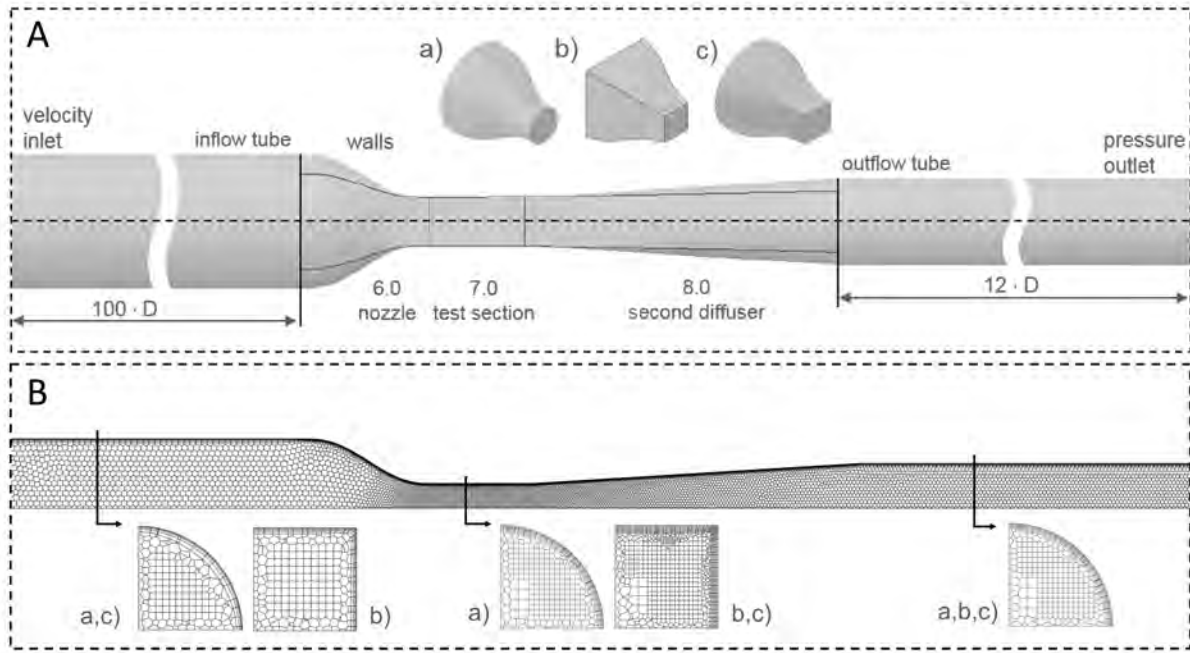


Figure 3 A) Computational domain for the simplified wind tunnel setup with a) circular shaped b) square shaped c) transitional nozzle geometry and B) illustration of the applied unstructured mesh

Nozzle Design

Numerous studies have been made to determine optimum nozzle geometries for wind tunnel application (Morel, 1975; Bell and Mehta, 1988; Brassard and Ferchichi, 2005). Main objectives were to avoid flow separation and to achieve high flow homogeneity. Bell and Mehta (1988) suggested a polynomial fifth order according to Equation 1 for the contraction design.

$$h(x) = \left[-10 \cdot \left(\frac{x}{L}\right)^3 + 15 \cdot \left(\frac{x}{L}\right)^4 - 6 \cdot \left(\frac{x}{L}\right)^5 \right] \cdot (H_i - H_o) + H_i \quad (1)$$

Here H_i and H_o designate the height of the contraction inlet and outlet over the contraction length L . This widely used approach for the design of wind tunnel contractions was initially applied for a nozzle with a rectangular cross section. The proposed polynomial satisfies the overall design criteria with the exception that the inlet curve radius should be much greater than the outlet radius. Brassard and Ferchichi (2005) suggested the transformation of the fifth order polynomial curve to overcome this restriction. However within this present study the polynomial fifth order according to (Bell and Mehta, 1988) is used as a first approach for the contraction of all three nozzle geometries for comparison. With the approach outlined the nozzle geometry for the fully circular and mostly square shaped setups were constructive generated by rotation and extrusion respectively. Hereby the size of the inlet and outlet cross-section area and therefore the contraction ratio was maintained approximately equal compared to the open test section configuration. In contrast the nozzle with a transitional cross-section was generated by a loft function. For this purpose an additional contraction curve for the diagonal plane was required and computed using Equation 1 with the half diagonal length of the square shaped test section as contraction outlet height H_o as illustrated in Figure 4. The contraction ratio was again maintained equal compared to the configuration with open test section.

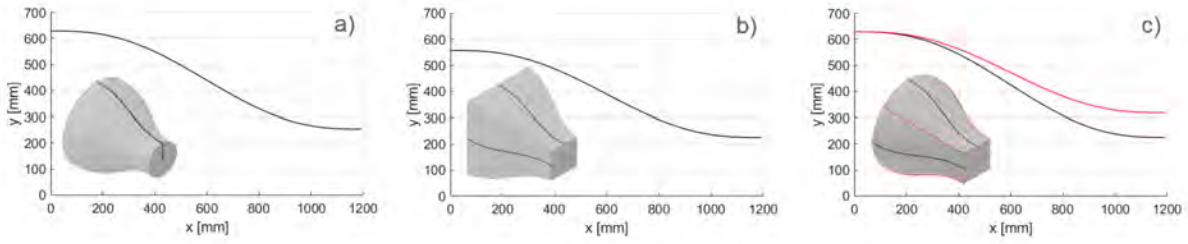


Figure 4 Nozzle geometries generated by a) rotation b) extrusion c) loft function

Homogeneity of Flow Quantities

Ideally the flow in the test section outside the boundary layer should be time-independent and uniformly parallel to the centerline. However since real tunnel application do not reach this state an acceptable value for the velocity variation across the test section often quoted lies within the range of 0.2 - 0.3% (Barlow et al., 1999). Provided that one can assume stationary flow a parameter derived from the standard deviation according to Equation 2 is used within this study for the evaluation of the flow homogeneity in the evaluation planes. The percentage velocity variation $|\Delta U|$ is calculated area weighted based on the numerical results using the local cell area A_{ci} normalized by the plane area A_p and the center velocity of the mid plane of the test section intended U_{cvmp} as reference.

$$|\Delta U| = \frac{\frac{1}{N-1} \cdot \sum_{n=1}^N \frac{A_{ci}}{A_p} \cdot |U_i - U_{cvmp}|}{U_{cvmp}} \cdot 100 \quad (2)$$

Since the measurement area for the planned wake measurements corresponds to only about one fifth of the cross section the evaluation of the flow homogeneity based on the described percentage velocity variation were carried out for the entire plane and a partial area with an edge length of approximately 45% of the test section edge length (Figure 5).

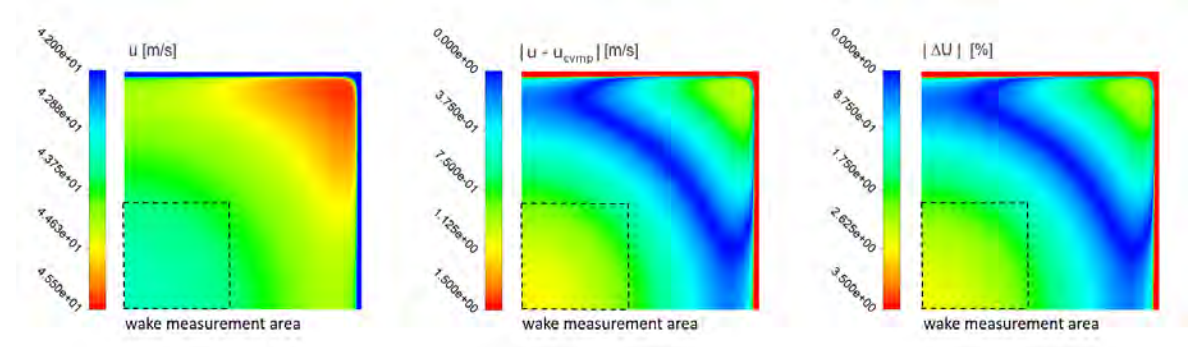


Figure 5 Schematic procedure for determining the percentage velocity variation on the contraction outlet plane

RESULTS AND DISCUSSION

For the evaluation of the flow homogeneity in the test sections seven planes with a uniform distance of 0.15 m each are considered as illustrated in Figure 6. In addition on the right side of Figure 6 the velocity profiles on the symmetry planes are illustrated. For the sake of completeness, the corresponding turbulence intensities are given in the appendix. However, since the influence of the setup on the turbulence intensity was hardly recognizable no further discussion on this flow quantity is provided. The evaluation of the flow homogeneity is done level by level using Equation 2. The corresponding percentage velocity variations for the entire planes are shown on the left side of Figure 7. The results show that as expected the fully circular setup shows the overall lowest percentage velocity variation within the test section. In contrast the mostly square shaped setup shows the lowest flow homogeneity. Especially in the test section inflow plane P_0 the nozzle with fully square cross section shows a significantly increased velocity variation in comparison. This is mainly due to the undesired flow acceleration in corner regions due to the intersecting circumferential edges and the accompanying local decreased flow volume within the contraction. From the plane P_1 on the percentage velocity variation between the square and circular setup remains approximately constant with a percentage deviation of $|\Delta U| \approx 0.4\%$. For the nozzle with transitional cross-sectional shape the percentage velocity variation shows qualitative the same course. In comparison to the mostly square setup however, the homogeneity can be increased over the entire length of the test section. Referring to

Figure 6 this can be attributed to the delayed corner influence and the resulting increased homogeneity in the test section inflow plane due to lower vorticity. Taking the trimmed area for wake measurements as a basis for the evaluation of the percentage velocity variation as illustrated on the right side of Figure 7 the results show a different behavior. Until the plane P_1 the setup with fully circular cross-section still shows the lowest percentage velocity variation and therefore the highest flow homogeneity. From plane P_2 on however, the percentage velocity variation of the transitional setup shows the overall highest flow homogeneity. This behavior can be attributed to the diffuser geometry. In all cases the maximum permissible diffuser opening angle was maintained equal. As a result the diffuser for the fully circular setup exhibits uniformly the maximum permissible diffuser opening angle over the circumference. In case of the square and the transitional setup however the maximum permissible diffuser opening angle only is present at the symmetry planes. Towards the corners the notional radius increases to a maximum value of $\sqrt{2} \cdot r$ which decreases the local diffuser opening angle and as consequence additionally the flow deceleration.

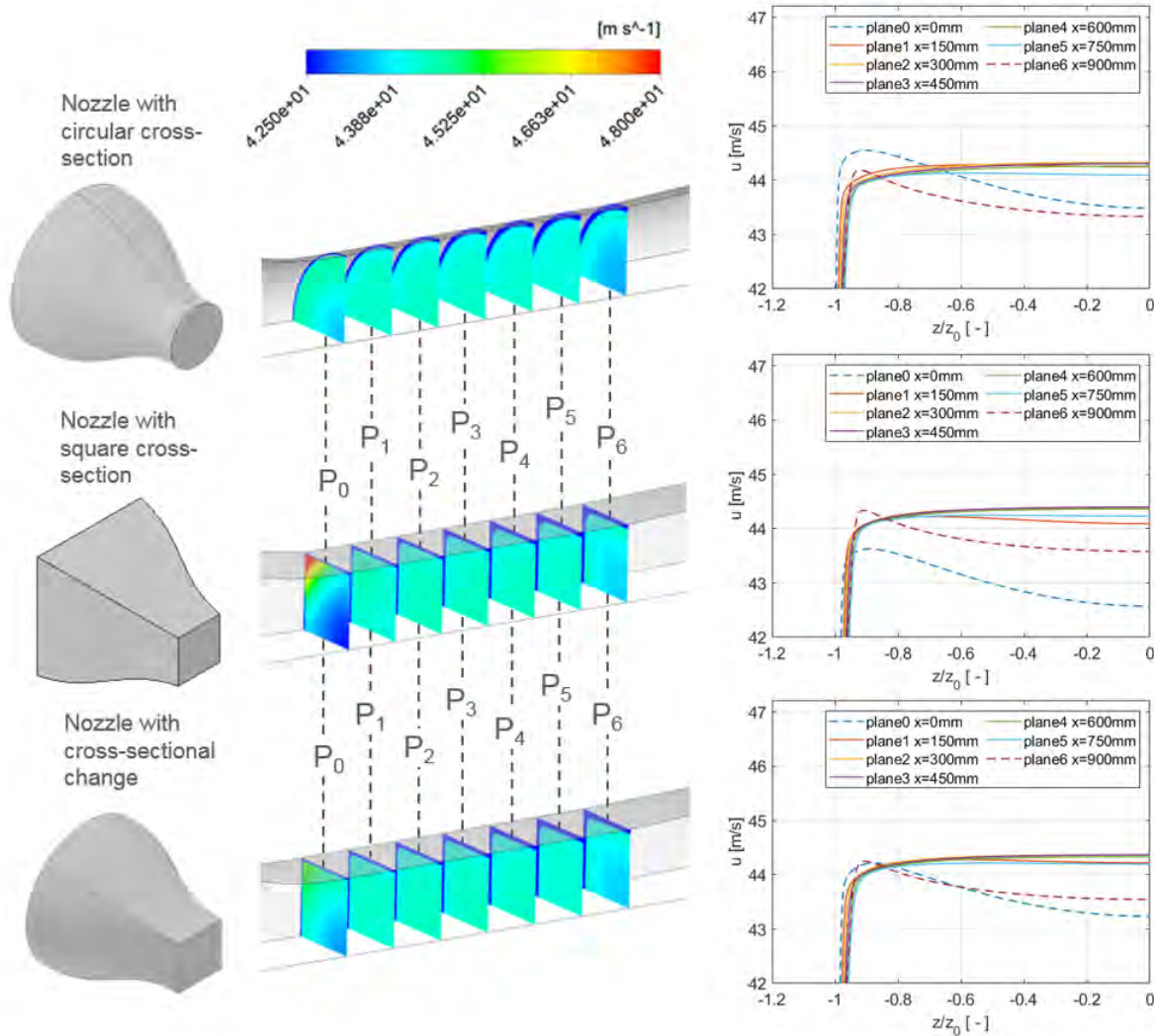


Figure 6 Velocity distribution on the evaluation and symmetry planes

Further according to the velocity distribution illustrated on the right side of Figure 6 it can be seen that the mostly square setup leads to an increased velocity variation in axial flow direction. Referring to the center velocity on the symmetry planes the maximum deviation amounts to $\Delta u \approx 1.8 m/s$ for the mostly square setup, $\Delta u \approx 1.0 m/s$ for the circular and $\Delta u \approx 1.1 m/s$ for the transitional setup respectively. A similar behavior can be seen when considering the static pressure distribution on the central axis as illustrated in Figure 8. The mostly square shaped setups in general provides the shortest region in the test section with a negligible pressure deviation. As a result, provided that these parameters are essential for the selection of a reasonable volume area for the performance of aerodynamic measurements, the transitional and circular setup provide a comparable higher range for the performance of reasonable measurements.

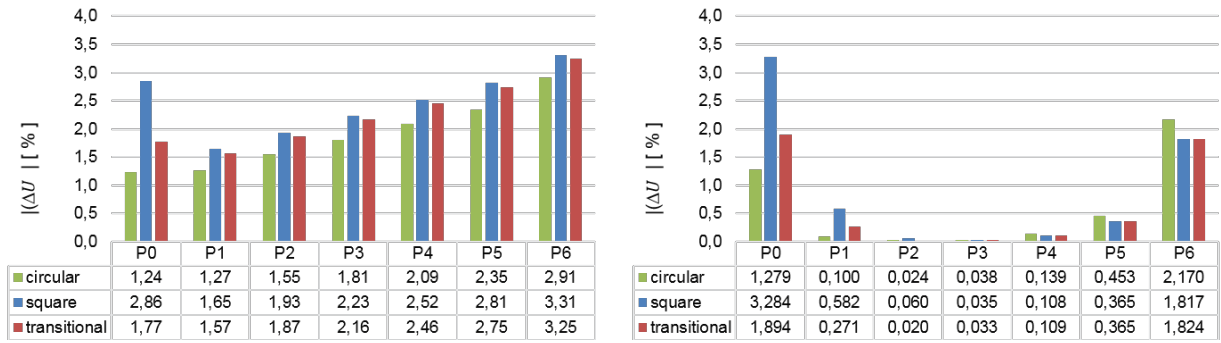


Figure 7 Percentage velocity variation of the entire (left) and partial evaluation planes (right)

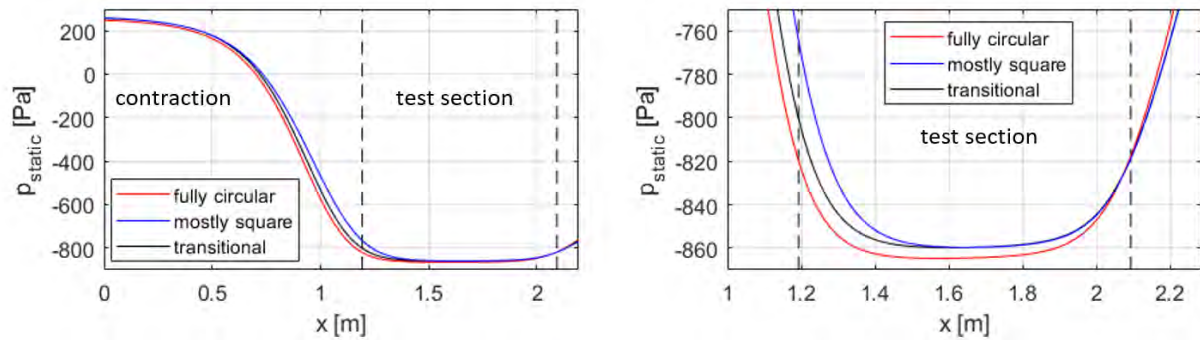


Figure 8 Static pressure distribution on the central axes

CONCLUSIONS

Open test sections are often unsuitable for determining precise lift and drag coefficient. Especially for high-lift models the different boundary conditions imposed by the open and closed test section configurations among others lead to a deviation of the local base pressure. Within this paper the authors present a design approach for an economically and aerodynamically optimized closure of a wind tunnel test section. According to the design requirements the cross-sectional shape of the test section was chosen to be square shaped. By including the necessary cross-sectional transition from circular to square within the nozzle geometry the number of new components to be manufactured can be reduced to a minimum. Meanwhile the flow homogeneity can be increased compared to a setup with fully square cross-section due to a delayed corner influence. This additional provides a longer region in the test section with negligible pressure deviation suitable for aerodynamic measurements. Furthermore, as for the transitional setup most components retain their circular cross-sectional shape, which causes less pressure losses, a decreased energy demand can be expected in comparison to the alternative mostly square setup. For this reasons the design approach outlined is economical beneficial for long term operation and preferable when high homogeneity is required in non-circular shaped test sections.

Presently the redesigned wind tunnel components for the approach outlined are in production. The reassembly and recommissioning will be put into practice in a timely manner which enables for experimental validation. However, as experience show that especially for closed loop wind tunnels numerical studies on strongly simplified models which dispense with corners, baffles, flow straightener, turbulence screens and swirls generated by the drive system are only partially suitable for validation based on experimental data a full model without the above mentioned simplifications will be implemented for the transitional setup.

NOMENCLATURE

| | | |
|----------|---|-------|
| A_{ci} | local cell area | m^2 |
| A_p | plane area | m^2 |
| A_1 | contraction inlet plane area | m^2 |
| A_2 | contraction outlet plane area | m^2 |
| C_R | area contraction ratio | — |
| D | diameter of the open test section | m |
| d_h | characteristic dimension of the closed test section | m |
| h_d | hydraulic diameter | m |

| | | |
|--------------|----------------------------------|-------|
| h | contraction height | m |
| H_i | contraction inlet height | m |
| H_o | contraction outlet height | m |
| l_{test} | test section length | m |
| U_i | local cell velocity | m/s |
| U_{cvmp} | center velocity of the mid plane | m/s |
| $ \Delta U $ | percentage velocity variation | % |
| x, y, z | axial coordinates | m |

References

- Barlow, J. B., Rae, W. H., Pope, A. and Pope, A. (1999), ‘Low-speed wind tunnel testing’, *New York: Wiley*.
- Bell, J. and Mehta, R. (1988), *Contraction Design for Small Low-speed Wind Tunnels*.
- Brassard, D. and Ferchichi, M. (2005), ‘Transformation of a Polynomial for a Contraction Wall Profile’, *Journal of Fluids Engineering* **127**(1), 183–185.
- Chen, T. and Liou, L. (2011), ‘Blockage corrections in wind tunnel tests of small horizontal-axis wind turbines’, *Experimental Thermal and Fluid Science* **35**(3), 565–569.
- Kramer, C., Gerhardt, H. and Janssen, L. (1986), ‘Flow studies of an open jet wind tunnel and comparison with closed and slotted walls’, *Journal of Wind Engineering and Industrial Aerodynamics* **22**(2), 115–127.
- Morel, T. (1975), ‘Comprehensive Design of Axisymmetric Wind Tunnel Contractions’, *Journal of Fluids Engineering* **97**(2), 225–233.
- Wetzel, D. A., Griffin, J. and Cattafesta, L. N. (2013), ‘Experiments on an elliptic circulation control aerofoil’, *Journal of Fluid Mechanics* **730**, 99–144.

APPENDIX

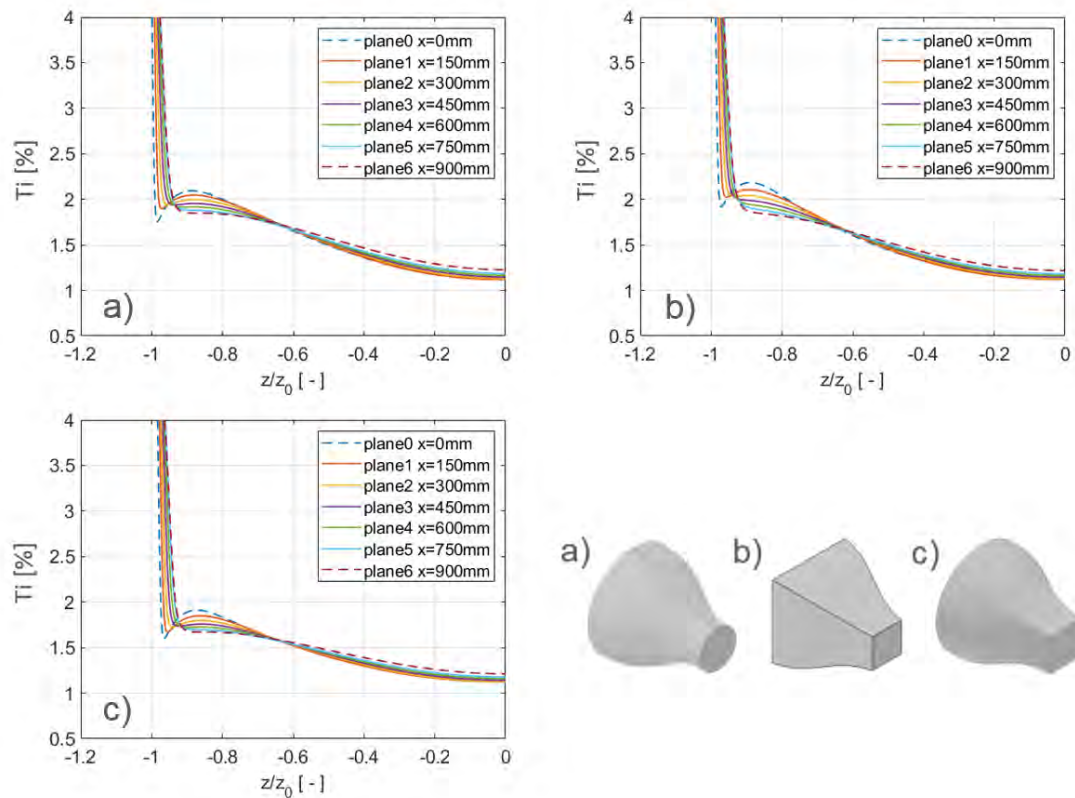


Figure 9 Turbulence intensity on symmetry planes for the a) fully circular b) mostly square and c) transitional wind tunnel setup